*Physical Modelling in Geotechnics*


# Free fall penetrometer for rapid site investigation for fish anchor

M.S. Hossain, Y.H. Kim & M.A. Mohiuddin
*Centre for Offshore Foundation Systems, Oceans Graduate School, The University of Western Australia, Australia*

N. Stark
*Virginia Tech, Charles E. Via, Jr. Department of Civil and Environmental Engineering, Blacksburg, USA*

S. Chow
*Department of Infrastructure Engineering, The University of Melbourne, Australia*

**ABSTRACT:** The free fall penetrometer (FFP) and fish anchor are deployed based on the same physics hinging on dynamic free fall through the water column, strike the sea/river floor at an impact velocity, and penetrate into the soil deposit until the momentum is depleted. This paper explores direct correlations between FFP and fish anchor penetration behavior towards utilizing FFP as a rapid site characterization tool for the fish anchor. A 1/15$^{th}$ scale instrumented model fish anchor was tested in the Swan River, Perth. The observations from the fish anchor tests were compared with existing cone FFP (FFcP) test results at the same site, and from a portable FFP (pFFP) test at a coastal site in the USA. The fish anchor and both FFPs were instrumented with accelerometers and pressure sensors. Surficial sediments at both sites consisted of predominantly soft clay. The achieved acceleration/deceleration and velocity profiles of the fish anchor and FFPs were consistent both in the water column and in riverbed/seabed. The fish anchor tip embedment depth estimated using the undrained shear strength profile deduced from the FFcP test data was in excellent agreement with measured embedment.

**Keywords:** embedment depth, fish anchor, free fall penetrometer, site characterization, velocity.

## 1 INTRODUCTION

The journey of using objects dynamically embedded in seabed sediments was launched in 1960s primarily for nuclear waste disposal purposes, followed by applications in naval mine countermeasure, seabed strength characterization, and deepwater anchoring systems. Amongst these applications, seabed characterisation using free fall penetrometers (FFPs) and deepwater mooring using dynamically installed anchors have gathered increasing attention in the last decade.

Various FFP designs, instrumentations, and analysis techniques have emerged (as summarised in Randolph et al., 2018). Most FFPs are instrumented with just accelerometers to measure the deceleration during penetration into the seabed, allowing indirect derivation of seabed strength (e.g. Colp et al., 1975). More sophisticated instrumentations (e.g. tip load cell, pore pressure transducers) have been incorporated in some FFPs to enable direct measurement of seabed strength and consolidation properties of soil (Steiner et al., 2012).

The dynamic seabed penetrometer concept was directly translated to anchoring solutions in the 1990s, addressing the offshore oil and gas industry identified need for a cost-effective and water depth insensitive anchoring solution for mooring floating facilities at remote deepwater locations. Dynamically installed torpedo (length, L = 12~17 m; dry weight, $W_d$ = 235~961 kN) and OMNI-Max (L = 9.15 m, $W_d$ = 383 kN) anchors have been commercially applied in clayey seabeds offshore Brazil and the Gulf of Mexico (Brandão et al., 2006; Shelton et al., 2011). Recently, the novel dynamically installed 'fish' anchor (L = 11 m, $W_d$ = 850 kN) has been proposed (Hossain et al., 2017; Chang et al., 2018), adopting a geometry taken from nature, for potential economic and safer mooring of oil and gas drilling platforms, wind turbines, and plastic collection nets in any water depths and seabed sediments.

This paper reports the results from two field tests conducted using the fish anchor and a portable FFP (pFFP) at clay dominated sites. Previously reported results (Vepulan, 2019) of a cone FFP (FFcP) at the same site of the fish anchor were compared. The aim is to explore direct correlations between FFP derived sediment data and fish anchor performance towards utilizing FFP as a rapid site characterization tool for the fish anchor. This is also logical and effective in terms of geotechnical design perspective, because currently seabed strength profiles are characterized by more time- and cost-intensive methods such as in situ quasi-static

cone penetrometer tests and/or laboratory triaxial tests. The strain rate induced during a quasi-static cone penetration test = penetration velocity/diameter = 20 mm/s / 35.7 mm = 0.56 /s and triaxial test = ~0.0017/72 = 2.32 × $10^{-5}$ /s. In contrast, a dynamically dropping object induces several orders of magnitude higher strain rate of e.g. 20 m/s / 2 m = 10 /s. As such, viscous strain rate dependent behaviour along with degree of remoulding (strain softening) and drainage/consolidation responses of a dynamically drop object is significantly different compared to those of a quasi-static test or laboratory test.

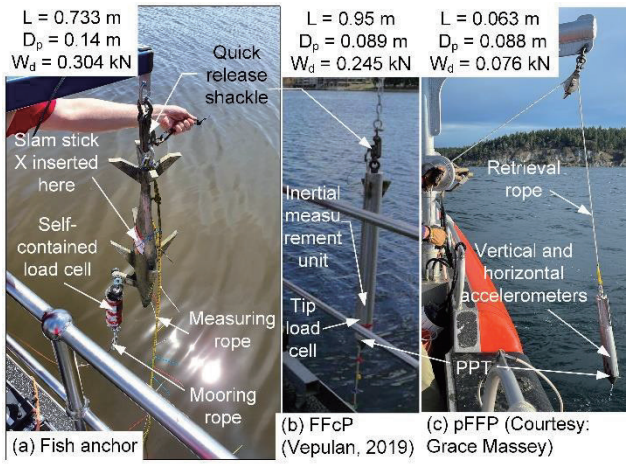


Fig. 1. Fish anchor, FFcP and pFFP test set-up.

## 2 FISH ANCHOR AND FFcP TESTS IN SWAN RIVER

The fish anchor was tested in the Swan River Perth. The riverbed consisted of soft clay. A 1/15$^{th}$ scale (L = 0.733 m, frontal projected area equivalent diameter, $D_p$ = 0.14 m, $W_d$ = 0.304 kN) scale model fish anchor was 3D printed from steel, with four body fins and four tail fins and the padeye welded onto the main body. The anchor body housed a commercial self-contained data logger, slam stick X (endaq.com). The slam stick comprised a ±16g micro-electro mechanical system (MEMS) accelerometer and a 2000°/s dual-axis gyroscope. On the same site, a series of FFcP tests was reported by Vepulan (2019). The FFcP (with 3 small tail fins) was 0.95 m in length (L) and 0.089 m in diameter (D = $D_p$). The dry weight was 0.245 kN ($W_d$). The cylindrical shaft housed an inertial measurement unit (consisting of accelerometers, gyroscope, data interface), a tip load cell, and two pore pressure transducers.

The experimental programs were carried out from a jetty and from a barge. The water depth was 1.4~3.6 m. The anchor or FFcP was suspended from its tail at a height above the water surface (as the water depth was limited), and then released by lifting the flap of a quick release shackle. Figures 1a and 1b show the anchor and FFcP ready to be released.

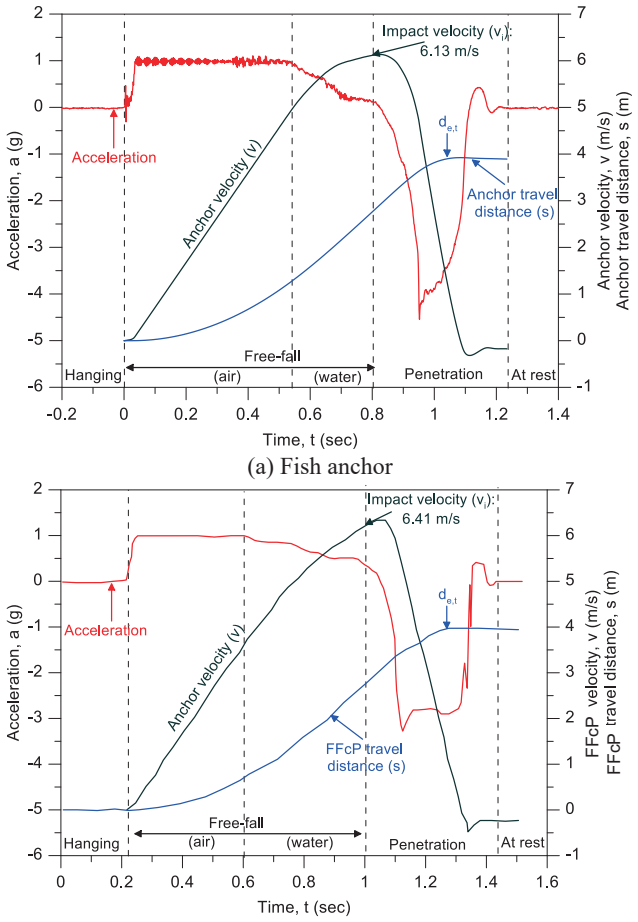


Fig. 2. Acceleration (a) and velocity (v) profiles from MEMS data.

Figures 2a and 2b show typical MEMS accelerometer data from the fish anchor and FFcP test, respectively. Prior to release (i.e. hanging), acceleration (a) was zero. During the free-fall stage in the air column, the acceleration remained constant at about 1g. After entering the water column, the acceleration started to reduce due to the hydrodynamic drag force. A more marked deceleration occurred after impacting the riverbed. The deceleration peaked at 4.5g (for fish) or 3.5g (for FFcP) prior to coming to the rest. By comparing Figures 2a and 2b, all phases of the profiles from the anchor and FFcP tests are consistent.

The acceleration (a) data were numerically integrated once to obtain the velocity (v) and twice to obtain the position or displacement, which are included in Figure 2, indicating tip embedment depth ($d_{e,t}$) and impact velocity ($v_i$). The resulting typical velocity-displacement profile and independent physical measurement of $d_{e,t}$ (straightening the measuring rope) are shown in Figure 3. The interpreted MEMS data in terms of $v_i$ and $d_{e,t}$ lie within 10% of the direct measurement. Again, the profiles are very consistent. The tip embedment depths are different due to different $W_d$, geometric configurations and $v_i$.

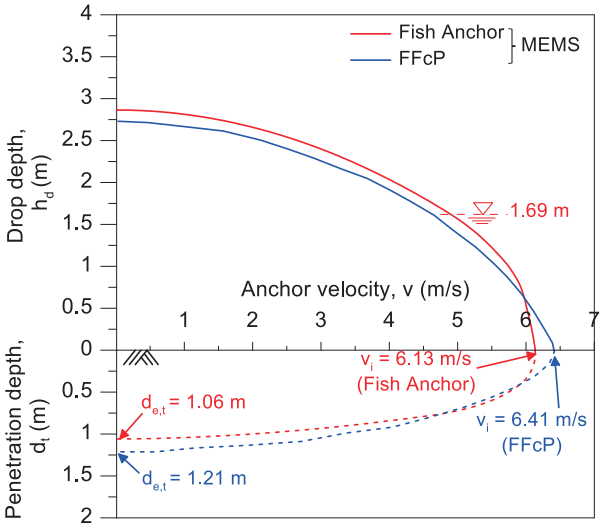


Fig. 3. Impact velocity ($v_i$) and tip embedment depth ($d_{e,t}$).

## 2.1 Undrained shear strength

The undrained shear strength ($s_u$) profile can be determined from FFcP test data using (i) direct method: the tip resistance and shaft load cell data, and/or (ii) indirect method: the measured acceleration/deceleration data and applying Newton's second law of motion (Chow et al., 2017). The direct method is presented as:

$$s_u = \frac{q_{cnet} - F_D/A_t}{R_{f,t}N_{kt}} \quad (1)$$

where $q_{cnet}$ is the static net cone tip resistance, $F_D$ is the drag resistance (Eq. 2), $A_t$ is the FFcP tip area, $R_{f,t}$ is the strain rate function for tip resistance (Eq. 2), and $N_{kt}$ is the cone resistance factor taken as 11.3. For the indirect method, the equation of motion (given below) is solved using the finite difference approach.

$$ma = W_s - F_t - F_s - F_b - F_D \quad (2)$$

where m and $W_s$ are the mass and submerged weight of the FFcP, a is the measured acceleration, $F_t$ is the bearing resistance on the base of the FFcP and fins, and $F_s$ is the frictional resistance on the FFcP shaft and fins:

$$F_t = R_{f,t}(s_u N_{kt} A_t), F_s = R_{f,s}(\alpha s_{u,avg} A_s),$$
$$F_D = \frac{1}{2}\rho_s C_D A_t v^2, \qquad F_b = \rho_s g V_s$$

$R_{f,t}$ and $R_{f,s}$ are the strain rate function calculated using the power law with power factor $\beta_t$ = 0.06, $\beta_s$ = 0.21, $A_t$ and $A_s$ are the bearing and surface area of the FFcP or fins, $\alpha$ = inverse of sensitivity = 0.22 (for Burswood clay; Low et al., 2011), $s_{u,avg}$ is the average shear strength over the FFcP embedded shaft or fins, $\rho_s$ is the submerged density of the soil = 487 kg/m$^3$ (Low et al., 2011), $C_D$ is the drag coefficient = 0.55, g is the Earth's gravitational acceleration, and $V_s$ is the volume of the soil displaced by the FFcP. More details on the soil parameter selection for Eq (2) can be found in Vepulan (2019). The strength profiles are plotted in Figure 4.

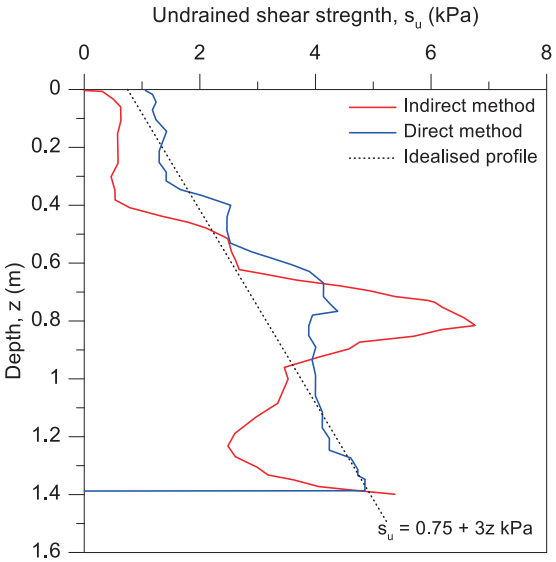


Fig. 4. Deduced undrained shear strength profiles from FFcP test.

The strength profile can be idealized as $s_u = s_{um} + kz$ = 0.75 + 3z kPa. For assessing anchor tip embedment depth, O'Loughlin et al. (2013) proposed a total energy-based expression

$$\frac{d_{e,t}}{D_p} = \left(\frac{E_{total} = \frac{1}{2}mv_i^2 + \acute{m}gd_{e,t}}{k_{eff}D_p^4}\right)^{1/3} \quad (3)$$

where m and m′ are the mass and effective mass of the anchor. Equation 3 gives $d_{e,t}$ = 1.2 m for $v_i$ = 6.13 m/s, which is consistent with the measured $d_{e,t}$ of 1.06 m (see Figure 3). The estimated $d_{e,t}$ values for various impact velocities are listed in Table 1.

Table 1. Estimated fish anchor tip embedment depth, $d_{e,t}$ (m).

| FFP | Site | $s_u$ kPa | $v_i$ = 6~6.13 m/s | $v_i$ = 10 m/s | $v_i$ = 15 m/s | $v_i$ = 20 m/s |
|---|---|---|---|---|---|---|
| FFcP | Swan River | 0.75+3z | 1.20 | 1.60 | 2.00 | 2.46 |
| pFFP | Sequim Bay | 0.5+1z | 1.79 | 2.34 | 2.97 | 3.56 |

## 3 PFFP TESTS IN SEQUIM BAY

Portable free fall penetrometers (pFFPs) have been deployed for rapid surficial (sediment depth ≤ 1 m) seabed/riverbed characterization for decades. For comparison, results from the pFFP BlueDrop are presented. This pFFP has a somewhat streamlined shape for application in energetic environments and to reduce side friction and drag, and thus, aligns well with the geometric concept of the fish anchor. It has maximum diameter of D = $D_p$ = 0.088 m, length L = 0.063 m and weight $W_d$ = 0.076 kN; with the conical tip option used in this example. It houses five vertical accelerometers and two horizontal accelerometers. A 2 MPa PPT is located just behind the cone at $u_2$ position.

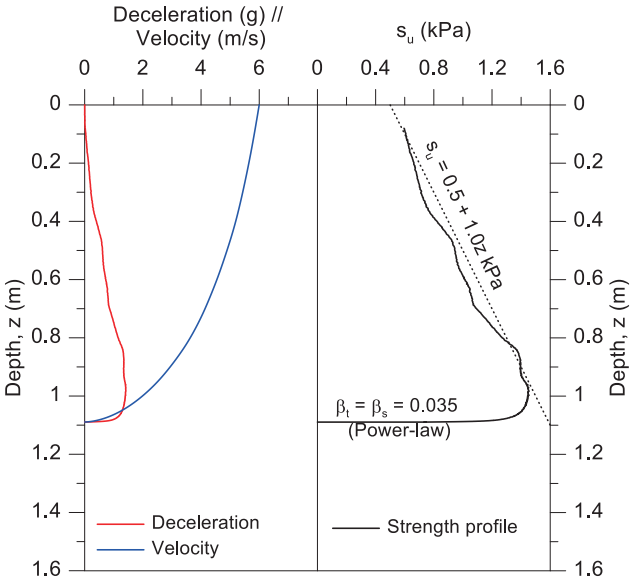


Fig. 5. Deceleration, velocity and undrained shear strength profiles from pFFP test.

An example collected most recently during a larger survey in Sequim Bay, Washington, USA, is presented here. The site consisted of soft fine-grained sediments, and had a water depth of ~ 35 m. The pFFP was deployed through release by hand. The pFFP was left in the seabed for some seconds before being retrieved. After impacting the seabed, the velocity and deceleration profiles are shown in Figure 5. The deceleration continued to ~1.5g prior to coming to the rest. The impact velocity was about $v_i$ = 6 m/s and the tip embedment depth $d_{e,t}$ = 1.1 m. Overall, the observed motion recordings for the pFFP match the observations for the fish anchor.

The undrained shear strength profile was deduced using the indirect method in Equation 2 with $\beta_t = \beta_s$ = 0.035 and $N_{k,t}$ = 12. The results were found to match with vane shear tests performed on the cored samples. The strength profile can be idealized as $s_u$ = 0.5 + 1z kPa. In this site, the fish anchor embedment depth can be estimated using Equation 3 as $d_{e,t}$ = 1.79, 2.34, 2.97 and 3.56 m for $v_i$ = 6, 10, 15 and 20 m/s; as listed in Table 1.

## 4 CONCLUSIONS

This paper reports the results from (i) the novel fish anchor tests in the Swan River, Perth; and (ii) the portable free fall penetrometer (pFFP) BlueDrop tests in Sequim Bay, Washington, USA. Previously reported results from the free fall cone penetrometer (FFcP) tests in the Swan River are compared. The following conclusions can be drawn from the results presented.

1) In the water column and in the riverbed/seabed, the fish anchor and FFcP velocity and acceleration/deceleration profiles were found to be consistent.
2) The undrained shear strength profiles deduced from the FFP test data were used directly (without any strain rate or softening adjustments) to estimate the fish anchor tip embedment depth, with excellent agreement obtained with the measured data. The shear strength can also be used for assessing the capacity or designing the anchor for supporting a floating facility.
3) The comparison confirms that an FFP can be used as a rapid site characterization tool for the fish anchor.

## ACKNOWLEDGEMENTS

The fish anchor tests were conducted with support from a Woodside RiverLab Project and the Australian Research Council (ARC) through the Future Fellowship FT190100735. The first author is an ARC Future Fellow and is supported by the ARC Project FT190100735. The pFFP test was conducted with the funding from SERDP through grant MR21-C1-1265. This support is gratefully acknowledged, as is the assistance of Eric Hunstein in data processing.

## REFERENCES

Brandão, F.E.N., Henriques, C.C.D., Araújo, J.B., Ferreira, O.C.G. and Dos Santos Amaral. C. 2006. Albacora Leste field development-FPSO P-50 mooring system concept and installation. *Proc. Offshore Technology Conf.*, OTC18243.

Chang, K., Hossain, M.S. et al. 2018. Novel dynamically installed fish anchor – diving upon loading in calcareous silt. *Proc. Offshore Technology Conf.*, Houston, OTC28901.

Chow, S.H., O'Loughlin, C.D., White, D.J., & Randolph, M.F. 2017. An extended interpretation of the free-fall piezocone test in clay. *Geotechnique*, 67(12), 1090-1103.

Colp, J.L., Caudle, W.N. and Schuster, C.L. 1975. Penetrometer system for measuring in situ properties of marine sediment. *Proc. IEEE Ocean '75*: 405-411.

Hossain, M.S, Kim, Y.H., Shim, J.U. and Ryu, M.C. 2017. *Anchor for deep seabed*. Korea Patent Application No. 10-2017-0018688.

O'Loughlin, C.D., Richardson, M.D., Randolph, M.F. and Gaudin, C. 2013. Penetration of dynamically installed anchors in clay. *Géotechnique* 63(11): 909-919.

Low, H.E., Maynard, M.L., Randolph, M.F. and DeGroot, D.J 2011. Geotechnical characterisation and engineering properties of Burswood clay. *Géotechnique* 61(7): 575-591.

Randolph, M.F., Stanier, S.A. et al. 2018. Keynote Lecture: Penetrometer equipment and testing techniques for offshore design of foundations, anchors and pipelines. *Proc. 4th Int. Symp. on Cone Penetration Testing (CPT'18)*: 3-23.

Shelton, J.T., Nie, C., Shuler, D., 2011. Installation penetration of gravity installed plate anchors-laboratory study results and field history data. *Proc. Offshore Technology Conf.*, Houston, OTC22502.

Steiner, A., L'Heureux, J.-S. et al. 2012. An in-situ free-fall piezocone penetrometer for characterizing soft and sensitive clays at Finneidfjord. *Submarine Mass Movements and their Consequences*: 99-109. Dordrecht, the Netherlands: Springer.

Vepulan, S. 2019. Characterization of soil strength in the Swan River using a free-falling cone penetrometer. Masters thesis, The University of Western Australia.